Synthesis, characterization and catalytic activity of highly dispersed Mo-SBA-15

J.A. Melero[a]*, J. Iglesias[a], J. M. Arsuaga[a], J. Sainz-Pardo[a], P. de Frutos[b] and S. Blazquez[b]

[a] Department of Chemical and Environmental Technology. ESCET. Universidad Rey Juan Carlos. C/ Tulipán s/n, E-28933. Móstoles. Madrid. Spain.

[b] Research Center of Repsol-YPF. E-28931. Móstoles. Madrid. Spain.

Published on:

Applied Catalysis A: General 331 (2007) 84-94

doi:10.1016/j.apcata.2007.07.031

Keywords: molybdenum; mesoporous; SBA-15; epoxidation; organic hydroperoxides

* To whom correspondence should be addressed.

juan.melero@urjc.es

Ph. +34 91 488 7087. Fax +34 91 488 7068

Summary

Molybdenum-containing SBA-15 materials have been prepared using a co-condensation method with a wide range of metal loadings under acidic conditions and using non-ionic surfactants. These materials display good catalytic activity in the epoxidation of olefins with alkyl hydroperoxides, being the catalytic activity correlated with the nature of supported molybdenum species. The immobilized metal species show different stabilities against leaching depending on their nature. Reutilization catalytic tests indicate that some fraction of the molybdenum show a high stability and it seems to be responsible for the major part of the catalytic activity of these materials. Stable molybdenum species use in a very efficient manner the alkyl hydroperoxide in the epoxidation of olefins whereas leached species leads to non-oxidative consumption of the oxidant and promote secondary reactions.

1. Introduction

The epoxidation of olefins is an important industrial chemical area as evidences the variety of oxirane production processes at industrial scale: the Ag-catalyzed ethylene oxidation [1], the chlorohydrin process [2], the hydrogen peroxide process [3] and the hydroperoxide process [4]. Several features related to the range of applicability, waste production and reagents availability [5 – 7] makes the hydroperoxide process the most extended industrial procedure for the synthesis of oxiranes, others than ethylene oxide, in presence of catalysts [7]. As main advantage, this process shows a low production of waste but its profitability depends on the market of the alcohol resulting from the hydroperoxide conversion [6] which links the success of the process to the efficient use of the oxidant.

Promoting the oxidation of olefins with organic hydroperoxides has been carried out using many kinds of catalysts [8], but most of the processes are based on molybdenum [9,10] and titanium species [11]. Unlike the titanium-based process, the molybdenum process uses homogeneous catalytic species. These soluble molybdenum catalysts show a very high catalytic activity and efficient use of the oxidant in olefin epoxidation [10] but display industrial problems associated to corrosion and deposition of the catalysts as well as the difficulty on its recovery. These troubles have promoted important efforts in the development of the heterogeneous counterparts of the homogeneous molybdenum catalysts [8],[12-14]. In this context, the recently developed mesostructured materials [15,16] have aroused great interest from scientists when heterogenizing homogeneous catalysts [17] like molybdenum-based oxidation catalysts. In this case, different heterogenization procedures have been described [18 - 21], but the most widespread methods for the immobilisation of heterometallic atoms are the post-synthetic surface grafting [22] and the direct synthesis procedures [23]. The first one usually involves the

use of an organometallic precursor which is reacted with the surface silanol groups to lead at least one Mo-O-Si bond [24]. In this way, the accessibility of the supported metallic species is ensured, but the risk of leaching of the active species is rather high. On the other hand, the direct synthesis methodology helps to get high dispersion degrees of the metal species, but their accessibility is not always achieved. The development of the oxo-peroxo route for the synthesis of Mo-functionalized MCM-type materials has improved this drawback [25], since the metal precursor acts as counter-ion in the interaction between the surfactant and the silicon species and thus, after the removal of the surfactant, the molybdenum atoms occupy surface locations. This protocol allows achieving high incorporation levels of the metal precursor [26-28] but, on the other hand, this procedure is only applicable when using ionic surfactants and the supported metallic species were partially leached during their first utilization in liquid phase oxidation catalytic tests, although further runs showed a much better behaviour regarding to the stability of the metal [28]. The synthesis of Mo-SBA-15, which is a quite more robust structure than the MCM-type, has been also achieved through this methodology by using a combination of surfactants (triblock copolymers and CTA^+X^-, where X^-= Cl^-, Br^-) [27,28]. The so-prepared materials have proved to be active in the oxidation of limonene and cyclooctene in presence of TBHP as oxidant but there is not information about their behaviour regarding to the efficient use of the oxidant and showed a high leaching degree during the reaction. Apart from these examples, few articles deal with other strategies to prepare molybdenum containing SBA-15 structures through co-condensation methodologies, probably because incorporation of heteroatoms into the matrix of SBA-15 type materials through direct synthesis procedures is a difficult task. The strong acidic media avoids the formation of Si-O-M bonds and destroys them when formed [29]. Nevertheless this technique has been widely applied

to the incorporation of several metal atoms, like Al [30], Ti [31,32] or Sn [33], to the structure of SBA-15 type materials with successful results. The key of the synthesis of these heteroatom-substituted SBA-15 materials has been the control of the pH of the synthesis media. The materials prepared using this technique show good dispersion of the active phase and high accessibility to the metallic sites. These investigations have prompted us to extend the application of this preparation technique to the case of molybdenum.

Herein, we present the synthesis, characterization and catalytic behaviour in the olefin epoxidation of molybdenum functionalized mesostructured materials prepared through a direct synthesis procedure under high acidic conditions with non-ionic surfactants and using ammonium heptamolybdate as metallic source. The preparation methodology involves a polyoxo route to achieve a moderate incorporation degree of the active metal, but leading to highly active supported molybdenum species. The activity of supported metal species has been correlated with their nature. Finally, this study has been made up with the analysis of the stability and reusability of the molybdenum-functionalized materials.

2. Experimental

2.1 Synthesis of Mo-SBA-15 materials

The synthesis of Mo-containing SBA-15 type materials has been tackled by using a modification of the procedure previously reported for the synthesis of Ti-SBA-15 [31]. Ammonium molybdate tetrahydrate [$(NH_4)_6[Mo_7O_{24}]\cdot 4H_2O$, Aldrich] and tetraethylorthosilicate [TEOS, Aldrich] were used as metal and silicon starting materials respectively. Pluronic 123 [$EO_{20}PO_{70}EO_{20}$, Aldrich] was used as structure directing agent. In a typical synthesis, 4.0 g of triblock copolymer were dissolved, under

magnetic stirring, in 125 mL of hydrochloric acid at room temperature. Two different acid concentration levels (0.5N and 1.9N) were used in order to determine the effect of the pH of the synthesis media on the incorporation degree of the metal species. After complete dissolution, the mixture was heated up to 40ºC and an appropriate amount of the molybdenum precursor was prehydrolized for at least 3 hours to give a clear yellow solution. Prehydrolysis step at such a high acid concentration has the purpose to depolymerize heptamolybdate species to form monomeric soluble molybdenum(VI) species [34, 35]. The yellow colouring of Mo/Pluronic-123/HCl aqueous solutions is caused by the complexation of Mo(VI) species by the poly(ethylene oxide) chains located in the corona area of the structure directing agent micelles [36]. In this way, the surfactant acts as a carrier of the metal species and favours their incorporation to the final siliceous material. After this, the silicon precursor was added to the resultant mixture in one step to lead a gel which was stirred for 20 additional hours. The resultant suspension was then transferred to an autoclave and hydrothermally aged at 100ºC under static conditions and autogenous pressure for 24 hours. During this stage the colouring of the solution turned from yellow to light blue, indicating a partial reduction of molybdenum species. The solids were recovered by filtration and air-dried overnight. As-made materials were calcined in air to remove the polymeric template. Calcination procedure was carried out at 550ºC during 5 hours under static air atmosphere to give the samples as white fine powders.

Mo-SBA-15 prepared by impregnation for comparison purposes, were synthesized as follows: In a typical synthesis, 1.0 g of calcined and outgassed SBA-15 was impregnated with an aqueous solution of the molybdenum precursor, using the needed concentration to achieve the desired Mo content assuming total incorporation. The wet

solid was then dried under vacuum and calcined in air under static conditions at 550ºC for 5 hours using a ramp step from rt to 550ºC during 5 hours.

2.2 Samples characterization

Bulk molybdenum contents of the synthesized materials were determined by Inductively Coupled Plasma - Atomic Emission Spectroscopy (ICP-AES). Typically, 100 mg of sample were dissolved in aqueous hydrofluoric acid. After dissolution, the sample was transferred to a 250 mL calibrated flask and diluted with water. An absorption standard solution of Mo (1000 mg/L in water) was used to calibrate the equipment. The limit of detection for molybdenum has been calculated accordingly to the IUPAC recommendations [37], being of 0.005% for this element and analytical conditions. Nitrogen adsorption/desorption isotherms at 77K were recorded using a Micromeritics TriStar 3000 porosimeter. The samples were previously outgassed in N_2 flow at 250ºC during 8 hours. Surface specific areas were calculated using the BET method. Pore size distributions were calculated using the BJH method assuming cylindrical pore geometry and using a Harkins-Jura type equation specifically fitted for SBA-15 materials [38]. The total pore volume was assumed to be that recorded at P/P_0=0.985. X-ray powder diffraction patterns (XRD) were collected on a Philips X'pert diffractometer using the Cu Kα line. The XRD data were recorded in the 2θ range from 0.6º to 5.0º with a step size of 0.02º for low angle analysis and in the 2θ range from 5.0º to 50º using a step size of 0.04º for high angle analysis. Diffuse reflectance UV-Vis spectra (DR UV-Vis) were recorded under ambient conditions in the wavelength range from 200 to 600 nm. DR UV-Vis spectra were collected using a Varian Cary-500. Raman spectra were recorded at room temperature using a LabRam HR spectrometer fitted with a Jobin-Yvon CCD detector using an excitation line at 632.8 nm from an

Helium Neon laser (source power: 11 mW). Transmission electron micrographs (TEM) and elemental analysis by EDS (spot beam analysis) were collected in a Philips Tecnai-200 electron microscopy operating a 200 kV.

2.3 Catalytic tests

The catalytic activity of the molybdenum-functionalized materials was assessed in the epoxidation of 1-octene with anhydrous tert-Butyl Hydroperoxide (TBHP, 5.5N in decane, Fluka) (TBHP:1-octene molar ratio of 1.2). To achieve proper anhydrous conditions, prior to their use in the catalytic oxidations, all the catalysts were outgassed by vacuum treatment at 250ºC overnight in order to remove the adsorbed water molecules which could interfere in the reaction results. The catalytic tests were carried out in a two-necked round bottom flask magnetically stirred and immersed in a temperature controlled bath under nitrogen atmosphere. All the reactions were performed for 6 h in the temperature range from 40 to 100ºC. In a typical assay both, the catalyst and 1-octene (1-octene: catalyst mass ratio of 12: 1; mass of catalyst 0.8 g) were loaded in the flask and the system was then warmed up to the reaction temperature. After heating, the oxidant was added in a single step by means of a syringe. Under the reaction conditions, epoxide was the major product, though in some experiments low contents of octanediol were also detected. The peroxide conversion (X_{TBHP}) was calculated by iodometric titration whereas the content of the rest of the products were quantified by gas chromatography analysis. Besides the conversion of the reactants, several other reaction parameters have been used for the comparison of the activity obtained using different catalysts. The definitions of the reaction parameters are as follows: Selectivity of the catalyst towards 1,2-epoxyoctane (S_{Epox}) is assumed to be the proportion of transformed 1-octene to lead epoxyoctane; the oxidant efficiency (η_{TBHP}) is the proportion of converted oxidant used in the formation of the oxirane;

turnover frequency (TOF) has been defined as the number of moles of produced epoxide divided by the number of moles of molybdenum added within the catalyst and by the reaction time (expressed in hours). The molybdenum leaching extension during the epoxidation tests, as well as the catalytic behaviour of leached species in the epoxidation have also been evaluated. The first parameter was determined by direct measurement of the molybdenum concentration in the reaction media after the filtration of the catalyst. The catalytic effect of the leached species was determined by monitoring the product distribution and oxidant conversion of an epoxidation reaction media after filtering the catalyst. Recycling tests were carried out by recovering the catalyst after reaction by filtration, followed by a washing step with ethanol and vacuum drying at 250ºC. In this way, all the chemicals that remained adsorbed onto the surface of the catalysts were completely removed.

3. Results and Discussion

3.1. Physicochemical characterization

3.1.1. Molybdenum content

Table 1 summarizes the synthesis conditions used for the preparation of different molybdenum-containing SBA-15 materials as well as their physicochemical properties regarding to the textural and structural parameters. In order to obtain different metal loadings on the mesostructured materials, the molybdenum content loaded in the initial gel for the synthesis of Mo-SBA-15 materials has been varied in the Si/Mo range from 25 to 12.5 in molar basis. Additionally, two different levels for the concentration of the hydrochloric acid have been used (1.9N and 0.5N), since the incorporation efficiency of metallic species within the structure of SBA-15 materials strongly depends on the pH of the synthesis media [31,32].

Bulk chemical analysis indicates a direct relationship between the initial metal loading in the synthesis gel and the metal incorporation onto the final material, a behaviour which is repeated in both acid concentration levels. Anyway, the metal incorporation efficiency is lower than 60% for these syntheses as a consequence of the strong acid conditions used for the preparation of the mesostructured materials. As previously noticed, acid conditions does not favour the formation of Si-O-Metal bonds and destroys them when formed. Several authors have described molar H^+/Mo ratios above 2 lead to highly soluble molybdenum species [34, 35], which in final term difficults the incorporation of the metal to a silica matrix. Under the specific conditions employed in this study (H^+/Mo range from 30 to 230) the heptamolybdate starting precursor is assumed to be completely depolymerized and thus the incorporation of the metal species is a difficult task. On the other hand, the ligand behaviour showed by PEO chains in the tri-block copolymer surfactants acts in the opposite way, favouring the incorporation of molybdenum species to the as-made materials [36].

Besides, the analyses of the final metal contents confirm the strong dependence of the metal incorporation efficiency on the pH of the synthesis media so that, the higher acid concentration, the lower metal incorporation. Thus, when using a stronger acid media ([HCl] = 1.9N; samples S1 – S3) the metal immobilization efficiency values are in the range 20-30% whereas using milder acid conditions ([HCl] = 0.5N; samples S4 – S6) leads to an increase of this parameter up to 50-60%. Anyway, the low metal incorporation efficiencies are, in this case, not only due to the aggressive acid conditions which lead to complete depolymerization of ammonium molybdate, but also because of the oxidation state of the molybdenum in the metal precursor. The atom geometry of Mo(VI) does not allow an isomorphic substitution of the silicon atoms, in other words, the metal cannot be incorporated into a silica matrix replacing a silicon

atom. Taking this into account, and bearing in mind that the poly(ethylene oxide) chains of the surfactant complex the Mo(VI) ions [36] the incorporation of molybdenum atoms must be placed necessarily through the reaction of Mo(VI) ions with structural defects, mainly located in the interface between the silica and surfactant micelles. Under these conditions, the final molybdenum species in the catalyst might be accessible by the reactants after surfactant removal. Thus, the proper tuning of the initial metal loading and the acid concentration has allowed preparing a whole collection of molybdenum-functionalized SBA-15 materials with metal contents varying from 0.9% to 4.0% in weight basis.

3.1.2. Nitrogen adsorption at 77K and XRD

The textural and structural parameters for the molybdenum containing SBA-15 materials, as well as a pure siliceous SBA-15 material, used as reference, have been evaluated by means of nitrogen adsorption analyses and X-ray diffraction. All the samples show surface area, pore sizes and total pore volume values which are typical from the SBA-15 topology. In principle, there is no clear trend in the dependency of any of the textural parameters on the molybdenum content of the samples. In fact, the 100 reflection in XRD analyses is located at quite similar angle values for all the tested materials, which means the incorporation of the metal to the silica does not influence the interplanar spacing of the SBA-15 structure. This parameter is usually modified when insertion of metal species within the silica matrix of mesostructured materials because of the different lengths of M-O and Si-O bonds [30, 32]. Thus, the invariability of the d_{100} lattice indicates that the molybdenum species are not incorporated inside the pore walls of the mesostructured materials but probably located at accessible positions over the channel surface as above mentioned.

Figure 1 displays the N_2 adsorption-desorption isotherm, pore size distribution in the mesoscopic range and X-ray diffraction pattern, recorded at low and high angle values, achieved for sample S6. This material has been taken as example among the prepared Mo-SBA-15 materials to illustrate the effect of the molybdenum on the structure of SBA-15 materials because of its high metal content should influence in a stronger way, on both the isotherm and the XRD pattern. The isotherm shape is of type-IV, according to the IUPAC classification which includes most of the mesoporous materials. The H1-type hysteresis loop, typical from SBA-15 materials, is also clearly evident, and the pronounced steep in the adsorption branch of the isotherm indicates a narrow pore size distribution which is typical of a well-ordered mesostructured materials. Regarding to the XRD pattern recorded for this sample, high angle reflections are completely missed, except the background signal caused by amorphous silica. This indicates a complete absence of crystalline domains of molybdenum oxide or, if present, the crystal sizes are too small to be detected by X-ray diffraction. On the other hand, intense signals are present at low angle values leading to a diffraction pattern characteristic of the p6mm symmetry of the hexagonal array of pores in the SBA-15 topology. The presence of three clear reflections, corresponding to the 100, 110 and 200 symmetries, is indicative of the high ordering achieved in the mesoscopic range. The rest of the materials show similar nitrogen adsorption isotherms and X-ray diffraction patterns to that showed in figure 1 confirming the good mesoscopic ordering for all the synthesized materials (see supplementary information).

3.1.3. UV-Vis diffuse reflectance and Raman spectroscopy

Figure 2 displays the DR UV-Vis spectra recorded for all the molybdenum-containing mesostructured samples as well as for MoO_3, used as reference, in the 200-600 nm

region. DR UV-Vis spectroscopy allows determining the structure of the supported metal species through the assignation of the different electronic transitions to different UV absorption bands. All the silica-based materials show similar UV spectra formed by three distinct absorption bands, located at 215, 240 and 290 nm. Since there is no significant absorption over 320 nm, signals which are attributed to the electronic transitions in dense phases of MoO_3 [39] like those present in its corresponding spectra, we consider that the materials are free from bulk molybdenum oxide. This result suggests that supported molybdenum species are well dispersed onto the surface of SBA-15 materials. Bands located in the region 200-250 nm are commonly attributed to the presence of isolated Mo^{6+} species as both mono- and dioxo-molybdenum species [24] and confirm the good dispersion of the metal. Nevertheless the signal centred at 290 nm is assigned to the electronic transitions caused by Mo-O-Mo bonds in oligomerized molybdate species [40], and it is more intense in the samples prepared under milder acid conditions ([HCl] = 0.5N; Figure 2, samples S4-S6). Although the pH of the media can vary the speciation of molybdenum species [41] the similarity of the DR UV-Vis spectra achieved for samples S3 and S4, having the same metal loading after synthesis but synthesized at different acid level, indicates, in this case pH has a limited influence on the final form of the supported molybdenum species, probably as consequence of the extremely high H^+/Mo ratio used for the synthesis of all of the materials. This is a feasible conclusion since the lowest acid concentration among all those employed in the hydrolysis of the molybdenum starting material is enough to lead a complete depolymerization of the heptamolybdate ion [34,35]. Anyway, as it has already been pointed out, decreasing the acidity of the synthesis media leads also to a higher incorporation degree of the metal species onto the final materials. Increasing the metal loading in the final material may influence the distribution of supported metal

species onto the SBA-15 materials since the higher molybdenum content, the higher intensity in the 290 nm signal. This is probably a consequence of the saturation of the metal anchoring points which causes the interaction between near metals atoms to yield polymolybdate species.

In order to step forward in the understanding of the nature of supported molybdenum species, DR UV-Vis spectra were transformed to calculate the energy edge values and the local structure of supported molybdenum species accordingly to the method described by Weber [42] (see supporting information). Thus, all the samples showed two different contributions to the overall UV spectra, one of them featured by an energy edge value around 4.0 eV and the second one showing energy edge values around 3.4 eV, depending on the molybdenum loading. These values are related to dimeric and oligomeric (heptamolybdate or related structures) molybdenum species. In this sense, the presence of dimeric molybdenum species is caused by the synthesis conditions, negative pH values and moderate molybdenum concentration [35]. On the other hand, the presence of heptamolybdate species could be attributed to two different causes: the presence of non hydrolyzed molybdenum precursor molecules or to the aggregation of molybdenum atoms because o the calcination of Mo-SBA-15 samples in presence of air atmosphere. Since this signal is already present for the as-made samples before calcination, we have assigned the origin of these species to the first of the causes. (See supplementary information for DR UV-Vis of as-made samples).

DR UV-Vis spectrum recorded for sample S1 has been compared with the spectra recorded for two Mo-SBA-15 samples prepared by incipient wetness impregnation and similar molybdenum content. These materials were synthesized by using silicomolybdic acid (SMA) and ammonium heptamolybdate as metal precursors. Because of molybdenum supported on silica usually leads to the formation of silicomolybdic acid

by calcination in presence of water, these molybdenum precursors have been selected in order to determine whether if the materials prepared by direct synthesis procedures contain SMA or not. Figure 3 shows the DR UV-Vis spectra recorded for sample S1, and the materials prepared by incipient wetness impregnation. All the materials were calcined prior to their analysis. The spectra recorded for the materials prepared by impregnation show a similar shape with almost the same contribution from each absorption bands in their corresponding spectra. On the other hand, sample S1 show a different spectrum, formed mainly by a band located at 210 nm whereas the bands located at 250 and 290 nm are less important in this case. The major signal is, as above mentioned, attributed to the electronic transitions in isolated molybdenum species. The presence of these species instead of silicomolybdic acid can be caused by the strong acid conditions used for the preparation of these materials which can lead to the hydrolysis of the molybdate precursor during both the hydrolysis and the ageing step to form monomeric molybdenum species [34, 35]. These species seem to remain attached even after calcinations of the material. In this way, it can be concluded that the material prepared by direct synthesis shows a higher dispersion degree of the molybdenum species than that achieved by incipient wetness impregnation.

Figure 4 depicts the Raman spectra recorded for several reference materials as well as highly molybdenum content sample S-6. In fact, due to the low metal loading and reduced particle size for the samples with lower metal contents, we were unable to achieve proper Raman spectra for the rest of the materials. The absence of the signals at 635 and 252 cm^{-1} in S-6 sample, present in the spectrum recorded for silicomolybdic acid, indicates a low amount of polymolybdate species. In the same sense, the magnification of the spectra recorded for sample S-6 shows a clear band formed by two contributions, one signal centred at 920 cm^{-1}, and a second one centred at 980 cm^{-1}.

Both signals are absent in the spectra recorded for pure silica SBA-15 sample, so that the bands are due to the presence of molybdenum species. In this sense, both contributions could be attributed to the symmetric stretching mode of Mo=O bonds in two different molybdenum species with different nature. Thus, the signal located at 920 cm^{-1} could be attributed to the presence of low-nuclearity molybdenum species. The low Raman shift achieved for this signal is related to the low metal loading [43]. On the other hand, the signal centred at 980 cm^{-1} is usually ascribed to M=O vibration modes in MoO_6 octahedra within polymolybdate domains [43]. These results are in agreement with those obtained by DR UV-Vis spectroscopy, where the presence of different molybdenum species supported on the SBA-15 silica materials has been detected.

3.1.4. Transmission electron microscopy

TEM images recorded for Mo-SBA-15 samples prepared with a range of metal loadings are shown in Figure 5. These micrographs show well-ordered hexagonal arrays of mesopores for all materials. No dense phases or MoO_3 crystallites have been detected in the external surface of SBA-15 particles. This fact is in fairly good agreement with the high homogeneity detected on the composition of the samples by EDS spot beam analyses, performed in-situ during the recording of the TEM images (see supplementary information). These results confirm the high dispersion of molybdenum achieved in these samples, even at the higher metal loading (S6 Sample), and they are consistent with those data obtained from the XRD analyses and DR UV-Vis spectroscopy.

Regarding to the mesoscopic morphology of the particles, slight differences are clearly evident for the samples with different molybdenum content. In this sense, increasing the metal loading leads to larger particles while keeping the hexagonal well-ordered array

of pores. This behaviour has been previously described in the case of Ti-SBA-1 materials, although in this latter, the material was obtained as spherical crystals [44].

3.2. Catalytic tests

The catalytic activity of molybdenum-containing SBA-15 materials has been assessed in the liquid phase epoxidation of 1-octene using anhydrous TBHP in decane as oxidant. Figure 6 depicts the influence of the temperature on the catalytic behaviour of the S4 material. As response variables the conversion of the reactants (X_{TBHP} and X_{Octene}), the selectivity of the catalyst towards the epoxide (S_{Epox}) and the efficiency in the use of the oxidant (η_{TBHP}) have been selected. The conversion of the reactants follows the classical relation with temperature, being higher when higher temperature is used. These results lead to, as expected, an increase of the turnover frequency calculated for each temperature. On the other hand both, the selectivity of the catalyst towards the epoxide and the TBHP use efficiency display similar values for 80ºC and 100ºC, which means an increase of the extent in the non-oxidative consumption of the hydroperoxide at the highest temperature. The measurement of the molybdenum content in the catalyst after reaction (data not shown) indicates that the increasing of the reaction temperature enhances the extension of the leaching of molybdenum species. These results have prompted us to set the reaction temperature for the rest of the catalytic tests on 80ºC, since the increasing of this parameter up to 100ºC does not improve so much the catalytic behaviour of the Mo-SBA-15 material but leads to an important increase in the extraction of the active metal content.

The results obtained in the epoxidation of 1-octene with TBHP over Mo-containing SBA-15 materials with different metal loadings are summarized in Table 2. Moreover, a study centred on the stability of the supported molybdenum species has also been

performed, involving the measurement of the molybdenum content of the catalyst before and after the reaction. For comparison purposes several reference reactions have been carried out in presence of different materials such as a pure silica SBA-15 material, silicomolybdic acid, ammonium heptamolybdate and molybdenum trioxide, and keeping the molar ratio 1-octene to molybdenum in close values to that of S1 sample. Pure siliceous SBA-15 material leads to negligible values of conversion of the octene and epoxide yield indicating the solid support employed for the synthesis of Mo-SBA-15 materials does not promote the epoxidation of terminal olefins. In the same sense, the conversion calculated for the oxidant is rather low which means the silica support does not promote a high non-oxidative consumption of the hydroperoxide.

The reaction carried out in presence of ammonium molybdate has resulted in moderate conversions of the reactants but excellent selectivity has been calculated for the catalyst in the transformation from 1-octene towards the corresponding oxirane. In the same way, the efficiency in the use of the oxidant is also satisfactory (90%). Taking into account that the homogeneous catalyst is formed by a polymolybdate ion, necessarily poly- and oligomeric molybdenum oxide species must promote the epoxidation of olefins in good yields and using the hydroperoxide oxidant in a very effective way. This conclusion is supported by the results obtained using bulk molybdenum oxide as catalyst in the oxidation of 1-octene. This material leads to lower reactants conversion than its homogeneous analogue, but excellent selectivities in the transformation of the substrate and the oxidant towards the epoxide have been accomplished, even higher than that achieved with ammonium molybdate. On the other hand, when using SMA as catalyst, the efficiency in the use of the oxidant highly decreases as well as the calculated turnover frequency for this chemical. The same low intrinsic catalytic activity has been detected for molybdenum trioxide, although in this latter, the oxidant is

employed in a very efficient manner. This difference between the soluble ammonium heptamolybdate and the insoluble SMA and MoO_3 can attributed to the different accessibility of the metal atoms in the molybdenum-based reference materials. Thus, in the case of the soluble ammonium molybdate almost all the molybdenum atoms are readily accessible, whereas in the case of bulk molybdenum oxide and SMA, part of the metal content is not accessible, leading to a decrease in the calculated TOF value. Anyway these results indicates that polymolybdates, even those bulk species present in MoO_3, show good catalytic behaviour in the epoxidation of olefins with alkyl hydroperoxides.

An additional reference run has been carried out in presence of a pure siliceous SBA-15 sample impregnated with ammonium heptamolybdate and subsequently calcined. The so-prepared material display moderate conversion of the olefinic substrate with excellent selectivity towards the epoxide. On the other hand, the efficiency in the use of the oxidant is really low since the conversion of the alkyl hydroperoxide is more than twice that obtained for the substrate. Besides this, the material prepared by impregnation show a low stability of the molybdenum species, since more than 80% of the original metal loading is easily leached during the catalytic test.

Regarding to the S1 material, this catalyst transforms the reactants in the same extension than the homogeneous catalyst does, although its efficiency in the use of the oxidant is lower. Interestingly, S1 sample shows a much greater turnover frequency than that achieved for all the reference materials with the exception of the homogeneous catalyst. This result might be a consequence of the high accessibility of the metal atoms in S1 sample because of the high dispersion degree achieved for the active phase as concluded from characterization results.

With regards to the influence of the molybdenum content on the catalytic activity of the SBA-15 materials, it is noticeable how the selectivity of the catalyst through the production of the epoxide, the efficiency in the use of the oxidant and the turnover frequency calculated for the catalyst are all reduced when increasing the molybdenum content within the catalysts. This particular catalytic behaviour seems to be correlated with, not only the metal loading in the catalytic tests, but also with additional variables like the nature of the supported molybdenum species, as well as the presence of solubilized molybdenum species in the reaction medium. Assuming that the polymolybdate species, as it has been previously noticed for the reference catalysts, drives the epoxidation reaction in a good efficient manner, supported polymolybdate species should lead to a similar catalytic behaviour as far as the nature of supported species is similar to that of the homogeneous catalyst. Taking this into account and bearing in mind that the increasing of the molybdenum content leads to an increase of the polymolybdate species onto the Mo-SBA-15 materials, the increasing of the molybdenum content should lead to a similarity between the catalytic behaviour of the heterogeneous molybdenum-based catalysts and that found for the reference catalysts. However, when increasing the metal loading, a lower efficiency in the use of the TBHP is achieved, which is just the opposite trend to that predicted. In this sense, not only the nature of the supported molybdenum species seems to influence the catalytic results but also leached molybdenum species can play an important role in the catalytic behaviour of the catalyst.

The evaluation of the metal content before and after catalytic tests has allowed determining the leaching extent of the molybdenum species for each catalyst as well as their influence on the catalytic activity of the Mo-SBA-15 materials. The increasing of the supported molybdenum content onto the SBA-15 materials leads to a higher

concentration of leached species in the reaction media but, interestingly, the proportion of leached molybdenum species with regards to the initial metal content seems to be rather similar between the tested materials. This result suggests that the proportion of unstable or labile metal species to the total molybdenum content supported onto the silica-based samples is equivalent for all of them.

The comparison between the results obtained in the assays on the stability of supported molybdenum with the catalytic results in the oxidation of 1-octene has resulted in a clear relationship between the amount of leached molybdenum species and the efficiency in the use of the oxidant, so that the higher leached molybdenum content, the lower efficiency in the use of TBHP. These results indicate leached metal species favour the non-oxidative consumption of TBHP, in other words, leached species promote the decomposition of the hydroperoxide molecules without catalyzing the oxidation of 1-octene towards the epoxide. Similar behaviour has been described for other molybdenum-based complexes which catalyze the decomposition of hydroperoxides, probably through a Haber-Weiss type reaction [45, 46]. This conclusion also explains the poor catalytic behaviour of impregnated Mo-SBA-15, whose low efficiency in the use of the oxidant could be related to the high leaching effect detected during the catalytic assay. Additionally, the increase of solubilized molybdenum species in the reaction medium also induces a significant decrease of the selectivity of the catalyst towards the corresponding epoxide. This means an enhancement of secondary reactions such as the hydrolysis of epoxyoctane to yield 1,2-octanediol. Moreover, the nature of leached species has to be completely different from polymolybdates like those at the homogeneous catalyst species, since their catalytic behaviour is opposite to that found for the soluble ammonium heptamolybdate.

In order to further evaluate catalytic activity and the nature of leached and remaining supported molybdenum species additional experiments were carried out. First, the activity of leached species was evaluated by monitoring the composition of a reaction media after catalyst removal by filtration. Second, the nature of leached species was evaluated by recording new DR UV-Vis spectra for the catalysts after being used in oxidation reactions. In the first assay, sample S4 was used in the catalytic epoxidation of 1-octene with TBHP as oxidant. The catalyst was filtered after 3 hours and the evolution of the composition of the reaction media was monitored for 3 additional hours. While the epoxide yield remained constant after filtration the alkyl hydroperoxide was consumed even after catalyst removal (see catalytic results in supplementary information). These results indicate the leached molybdenum species does not promote the epoxidation of the olefin but catalyse the non-oxidative consumption of the oxidant.

Regarding to the nature of the leached species, figure 7 shows the comparison between the spectra recorded for some Mo-SBA-15 materials before and after their use in the epoxidation tests. All the materials show the same evolution in their DR UV-Vis spectra: the decrease of the intensity of the signal located at 250 nm up to complete disappearance and the increasing of the relative intensity of the signal centred at 300 nm. These results indicate that isolated molybdenum species absorbing at 210 nm in UV-Vis seems to be stable and those correlated to the presence of the signal at 250 nm are easily extracted. On the other hand, supported isolated molybdenum and polymolybdate species (UV-Vis band centred at 290 nm) seem to be also stable and remain attached to the material after reaction. These results are also confirmed by the evaluation of the local structure of supported molybdenum species after epoxidation reactions. Thus, unlike oligomeric molybdenum species lead to almost the same energy

edge value (3.3-3.4 eV), and consequently the same local structure, less condensed molybdenum species lead to energy edge values around 4.3-4.5 eV which indicate the existence of monomeric molybdenum species. These displacements do not mean the transformation of dimeric molybdenum species into monomeric ones but, probably leached molybdenum species are those dimeric forms of the molybdates as previously stated. Thus, once dimeric molybdenum species have been removed during the catalytic tests, the UV-Vis spectrum of the stable monomeric forms of the molybdenum supported species is revealed.

With the purpose to assess the reusability of the molybdenum-functionalized catalysts and determining the catalytic behaviour of stable molybdenum species, new experiments, based on the reutilization of S1 catalyst, have been performed. Table 3 shows the results obtained in the reutilization tests carried out using this material. This sample has been selected for this study since it shows the higher catalytic activity per molybdenum centre as well as the maximum efficiency in the use of the oxidant. Reusing the Mo-SBA-15 material results not only in an increasing of the selectivity of the catalyst towards the epoxide but also improves the efficiency in the use of the oxidant. Additionally, the calculated parameter for the activity of the catalyst per metal centre (TOF) is greatly enhanced in each reutilization. These results do not mean supported molybdenum species become more active on each recycling test but the explanation is related to the stability of the metal species. Thus, a partial loss of the supported metal species is observed during the second reutilization but the leaching is negligible during the third run. Bearing in mind leached species promote the decomposition of the oxidant but not the epoxidation of the olefinic substrate, the reduction of this effect on each reutilization run leads to an increase of the intrinsic catalytic activity. In other words, while leached molybdenum species decreases the

efficiency in the use of the oxidant in the epoxidation of 1-octene and promote secondary reactions, remaining supported molybdenum species are the responsible of catalytic activity. The removal of labile Mo species, which are not active in epoxidation, reveals the true catalytic activity of those metallic sites stable and catalytically active in epoxidation. This catalytic result opens an interesting research field to be explored in the future in order to control the local structure of Mo species which finally will result in an improvement of the catalytic performance.

4. Conclusions

Mo-SBA-15 materials have been prepared through a direct synthesis procedure involving a polyoxo route. The prepared mesostructured materials show good mesoscopic ordering degrees, narrow pore size distributions and high dispersion of the metal oxide. The interaction occurring between the molybdenum precursor and the surfactant plays a crucial role in the metal incorporation degree under such high acid concentration. Different supported metal species have been detected onto the final samples and, although some of the immobilized molybdenum oxide is labile and easy to leach, the stable fraction of the active phase shows good catalytic behaviour in the epoxidation of olefins in presence of TBHP. The nature of both, stable and unstable metal species has been correlated with different atom environments through UV-Vis and Raman spectroscopies. Molybdenum leached species, which have been correlated to dimeric molybdates, are responsible of a decreasing in the oxidant efficiency and the presence of undesirable secondary reactions. Tuning the local structure of supported molybdenum species open an interesting research field to obtain Mo-SBA-15 materials displaying high metal stability and good catalytic performance in the epoxidation of olefins with alkyl hydroperoxides.

References

[1] R.E. Egbert, R. Heights, US Patent 2,693,474, (1954)

[2] (a) E. Bartholome, W. Koehler, G. Stoeckelmann, A. May, US Patent 3,886,187, (1975); (b) E. M. Jorge, US Patent 6,043,400, (2000)

[3] M.G. Clerici, A. de Angelis, P. Ingallina, US Patent 5,221,795 (1993)

[4] J. Kollar US Patent 3,351,635 (1967)

[5] R. M. Lambert, F.J. Williams, R.L. Cropley, A. Palermo, J. Mol. Catal. A 228 (2005) 27-33

[6] T.A. Nijhuis, M. Makkee, J.A. Moulijn, B.M. Weckhuysen, Ind. Eng. Chem. Res. 45 (2006) 3447-3459.

[7] A. Tullo, Chem. Eng. News 83 (2005) 7.

[8] U. Arnold, R. Serpa da Cruz, D. Mandelli, U. Schuchardt, J. Mol. Catal. A 165 (2001) 149-168

[9] R. Martos Calvente, J.M. Campos-Martín, J.L.G. Fierro, Catal. Commun. 3 (2002) 247-251.

[10] St.V. Kotov, E. Balbolov, J. Mol. Catal. A 176 (2001) 41-48

[11] J.K.F. Buijink, J.J.M. van Vlaandern, M. Crocker, F.G.M. Niele, Catal. Today 93-95 (2004) 199-204

[12] G. Grivani, S. Tangestaninejad, M.H. Habibi, V. Mirkhani, M. Moghadam, Appl. Catal., A 299 (2006) 131-136.

[13] L.-X. Dai, Y.-H. Teng, K. Tabata, E. Suzuki, T. Tatsumi, Chem. Lett. 29 (2000) 794-795

[14] M. Masteri-Farahani, F. Farzaneh, M. Ghandi, J. Mol. Catal. A. Chem. 192 (2003) 103-111

[15] J.S. Beck, J.C. Vartulli, W.J. Roth, M.E. Leonowicz, C.T. Kresge, K.D. Schmitt, C.T.-W. Chu, D.H. Olson, E.W. Sheppard, S.B. McCullen, J.B. Higgins, J.L. Schlenker, J. Am. Chem. Soc. 114 (1992) 10834-10843

[16] D. Zhao, Q. Huo, J. Feng, B.F. Chmelka, G.D. Stucky, J. Am. Chem. Soc. 120 (1998) 6024-6036

[17] A. Corma, Chem. Rev. 97 (1997) 2373-2419

[18] G.M. Dhar, G.M. Kumaran, M. Kumar, K.S. Rawat, L.D. Sharma, B. D. Raju, K.S. R. Rao, Catal. Today 99 (2005) 309-314

[19] S. Higashimoto, Y. Hu, R. Tsumura, K. Iino, M. Matsuoka, H. Yamashita, Y.G. Shul, M. Che, M. Anpo, J. Catal. 235 (2005) 272-278

[20] A. Sakthivel, J. Zhao, G.Raudashl-Sieber, F.E. Kühn, J. Organomet. Chem. 690 (2005) 5105-5112

[21] A. Sakthivel, J. Zhao, F.E. Kühn, Microporous Mesoporous Mater. 86 (2005) 341-348

[22] Q. Yang, C. Copéret, C. Li, J.M. Basset, New. J. Chem. 27 (2003) 319-323

[23] W. Zhang, J. Wangt, P.T. Tanev, T. Pinnavaia, Chem. Commun. 6 (1996) 979-980.

[24] J. Jurapatrakorn, M.P. Coles, T.D. Tilley, Chem. Mater. 17 (2005) 1818-1828

[25] J.-Y. Piquemal, J.-M. Manoli, P. Beaunier, A. Ensuque, P. Tougne, A.-P. Legrand, J.-M. Brégeault, Microporous Mesoporous Mater. 29 (1999) 291-304.

[26] J.-Y. Piquemal, E. Briot, M. Vennat, J.-M. Brégeault, G. Chottard, J.-M. Manoli, Chem. Commun. 13 (1999) 1195-1196

[27] E. Briot, J.-Y. Piquemal, J.-M. Brégeault, New. J. Chem. 26 (2002) 1443-1447.

[28] P.C. Bakala, E. Briot, L. Salles, J.-M. Brégeault, Appl. Catal. A 300 (2006) 91-99.

[29] W.-H. Zhang, J. Lu, B. Han, M. Li, J. Xiu, P. Ying, C. Li Chem. Mater. 14 (2002) 3413

[30] C. Calleja, J. Aguado, A. Carrero, J. Moreno Appl. Catal. A 316 (2007) 22-31

[31] J.A. Melero, J.M. Arsuaga, P. de Frutos, J. Iglesias, J. Sainz, S. Blázquez, Microporous Mesoporous Mater. 86 (2005) 364-373

[32] S. Wu, Y. Han, Y.-C. Zhou, J.-W. Song, L. Zhao, Y. Di, S.-Z. Liu, F.-S. Xiao, Chem. Mater. 16 (2004) 486-492

[33] P. Shah, A.V. Ramaswamy, K. Lázár, V. Ramaswamy, Microporous Mesoporous Mater. 100 (2007) 210-226

[34] J.J. Cruywagen, J.B.B. Heyns, Polyhedron, 19 (2000) 907-911

[35] R.I. Maksimovskaya, G.M. Maksimov, Inorg. Chem., 46 (2007) 3688-3695

[36] K.G. Vassilev, D.K. Dimov, R.T. Stamenova, R.S. Boeva, Ch.B. Tsvetanov, J. Polym. Sci., Part A: Polym. Chem. 24 (1986) 3541-3554.

[37] IUPAC. Analytical Chemistry Division. Pure Appl. Chem. 45 (1976) 99-103

[38] R. van Grieken, G. Calleja, G.D. Stucky, J.A. Melero, R.A. García, J. Iglesias, Langmuir 19 (2003) 3966-3973

[39] Z. Liu, Y. Chen, J. Catal. 177 (1998) 314-3240

[40] A. Duan, G. Wan, Z. Zhao, C. Xu, Y. Zeng, Y. Zhang, T. Dou, X. Bao, K. Chung, Catal. Today 119 (2007) 13-18.

[41] F.A. Cotton, C.A. Murillo, M. Bochmann, Advanced Inorganic Chemistry, sixth ed., John Wiley & Sons, New York, 1999.

[42] R.S. Weber, J. Catal. 151 (1995) 470-474.

[43] I. Shupyk, J.-Y. Piquemal, E. Briot, M.-J. Vaulay, C. Connan, S. Truong, V. Zaitsev, F. Bozon-Verduraz, Appl. Catal. A 325 (2007) 140-153.

[44] D. Ji, R. Zhao, G. Lv, G. Qian, L. Yan, J. Suo, Appl. Catal. A 281 (2005) 39-45.

[45] D. Damianov, Tanielan, Reac. Kinet. Catal. Lett. 21 (1982) 191-194

[46] A. Keller, J.M. Sobczak, R. Matusiak, J. Mol. Catal. A: Chem. 136 (1998) 115-125.

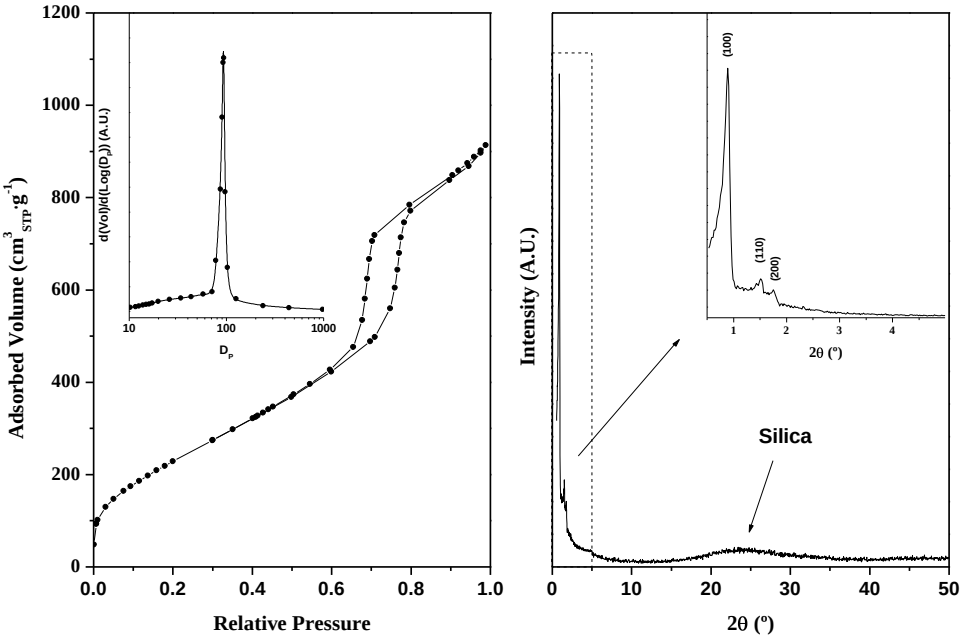

Figure 1.

J.A. Melero *et Al.*

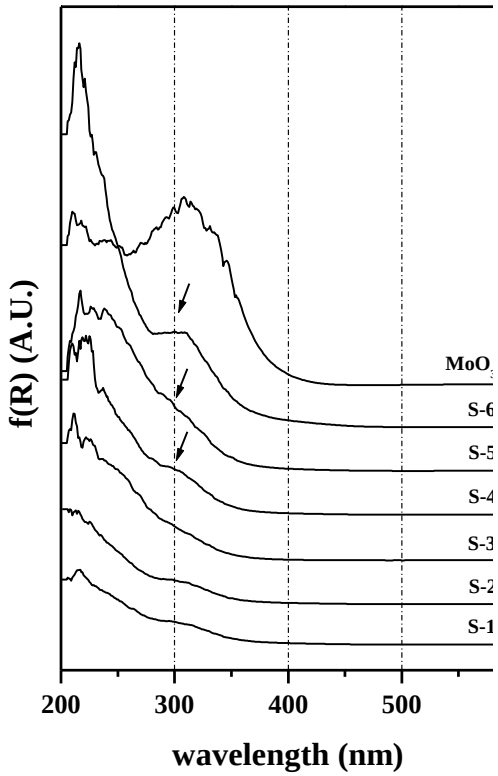

Figure 2

J.A. Melero *et Al.*

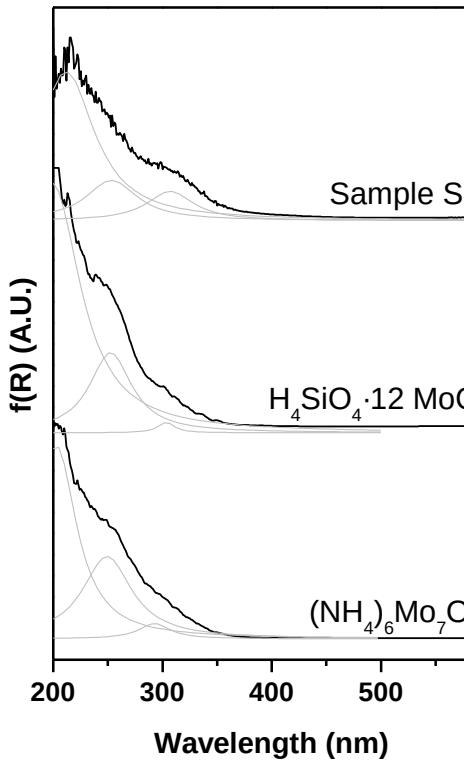

Figure 3

J.A. Melero *et Al.*

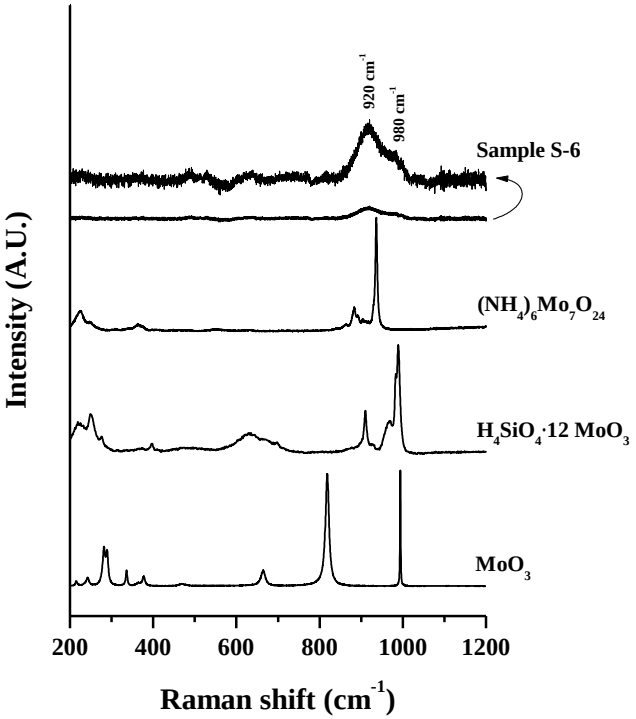

Figure 4

J.A. Melero *et Al.*

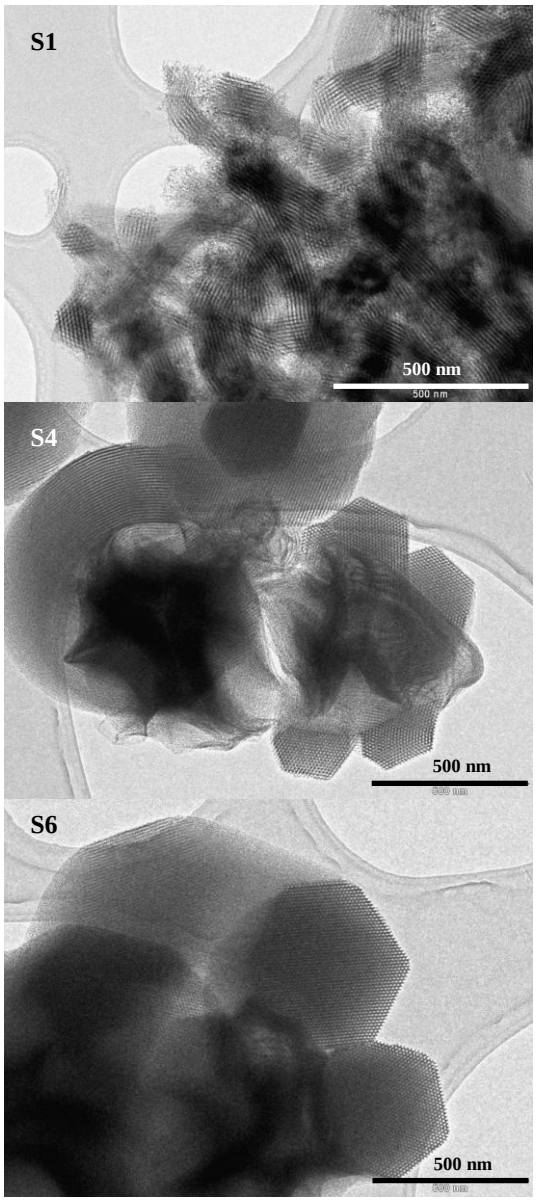

Figure 5

J.A. Melero *et Al.*

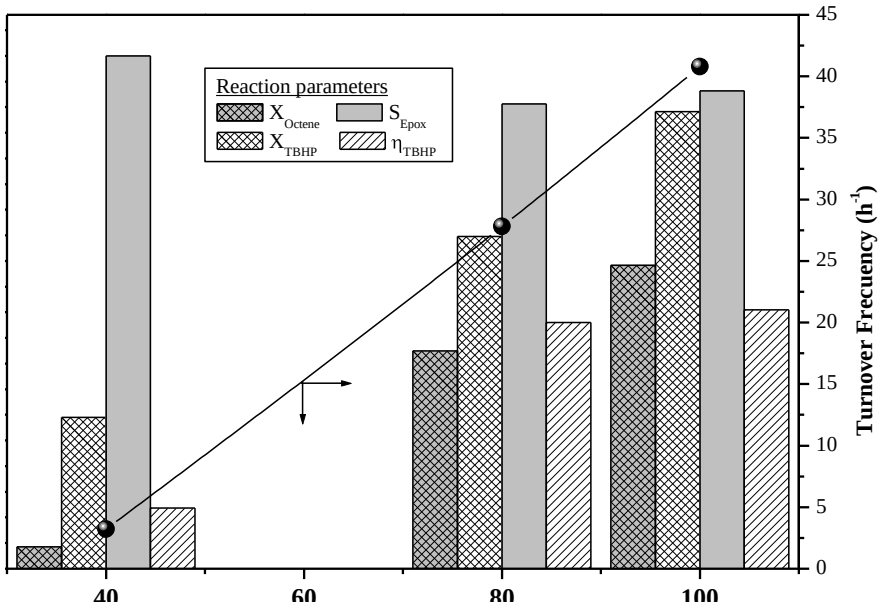

Figure 6

J.A. Melero *et Al.*

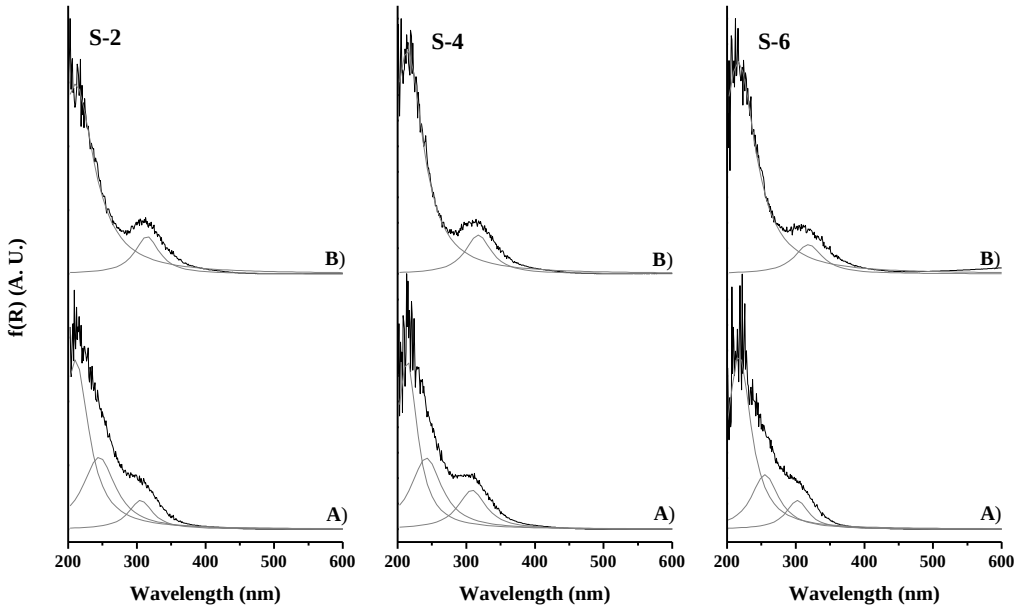

Figure 7

J.A. Melero *et Al.*

Figure Captions

Figure 1. Nitrogen adsorption-desorption isotherm, pore size distribution and X-ray diffraction pattern for sample S6.

Figure 2. DR UV-Vis spectra of Mo-SBA-15 with different metal loadings

Figure 3. DR UV-Vis spectra for molybdenum containing SBA-15 materials prepared by direct synthesis (S1) and wetness impregnation

Figure 4. Raman spectra of different Mo-containing materials.

Figure 5. TEM images recorded for Mo-SBA-15 with different metal loadings.

Figure 6. Oxidation of 1-octene with TBHP at different temperatures.

Figure 7. DR UV-Vis spectra of Mo-SBA-15 samples A) Before and B) After use in the epoxidation of 1-octene

Table 1. Physicochemical properties of Mo-functionalized SBA-15 materials.

Sample	Synthesis conditions			Composition			Textural Properties				
	$[Si/Mo]_0$ [a]	[HCl] / N	H^+/Mo	[Si / Mo] [b]	Mo (%) [c]	η (%) [d]	S_{BET} (m^2/g) [e]	D_P (Å) [f]	V_P (cm^3/g)	d_{100} (Å)	W_t (Å) [g]
SBA-15	---	1.9	∞	---	0.0	---	605	86.1	0.922	90.0	17.8
S-1	25.0	1.9	229	176	0.9	22.5	677	84.6	1.149	97.0	27.4
S-2	16.7	1.9	153	101	1.6	26.0	845	92.4	1.363	101.4	24.7
S-3	12.5	1.9	115	66	2.4	29.5	871	90.1	1.387	99.1	24.3
S-4	25.0	0.5	60	68	2.3	57.8	975	95.8	1.357	101.4	21.3
S-5	16.7	0.5	40	52	3.0	49.8	594	90.8	0.885	101.4	26.3
S-6	12.5	0.5	30	38	4.0	50.0	685	100.8	1.017	103.8	19.1

[a] Silicon to molybdenum atomic ratio in the initial gel mixture. [b] Silicon to molybdenum atomic ratio in the final material after calcination measured by ICP-AES. [c] Molybdenum content in % wt [d] Mo incorporation efficiency. [e] Determined by the BET method. [f] Calculated by the BJH method. [g] Wall thickness calculated from XRD experiments and N_2 adsorption analysis ($W_t=\{d_{100}\cdot 2/\sqrt{3}\}-D_p$)

Table 2. 1-Octene epoxidation with TBHP over Mo-SBA-15 [a]

Catalyst	Catalytic Results						Molybdenum stability			
	Oct:Mo (molar)	X_{Octene} [d] (%)	X_{TBHP} [e] (%)	S_{Epox} [f] (%)	η_{TBHP} [g] (%)	TOF [h] (h^{-1})	Mo_0 [i] (%)	Mo_f [j] (%)	Mo_{Leach} [k] (%)	Mo_{sol} [l] (ppm)
SBA-15 (SiO_2) [b]	∞	0. 8	7.9	1.5	0.1	---	---	---	---	---
$(NH_4)_6Mo_7O_{24}{\cdot}4H_2O$ [b]	1000	58.5	54.1	99.9	88.2	97.2	--	---	---	323
$H_4SiO_4 \cdot 12MoO_3$ [b]	1000	41.2	51.5	99.9	64.4	67.5	---	---	---	323
MoO_3 [b]	1000	28.6	24.2	99.9	96.4	45.8	---	---	---	---
SBA-15 / $(NH_4)_6Mo_7O_{24}{\cdot}4H_2O$ [b, c]	1100	40.2	84.2	99.7	33.6	68.3	0.90	0.18	80.56	218
S-1	1100	46.8	57.7	98.6	67.1	87.4	0.90	0.50	44.80	128
S-2	640	50.7	65.5	95.5	60.9	51.3	1.56	0.80	48.98	125
S-3	440	54.9	77.7	92.5	53.7	36.9	2.36	0.93	60.64	248
S-4	430	49.1	77.3	90.6	48.0	27.8	2.31	1.11	51.87	350
S-5	350	46.6	76.9	90.2	45.4	24.3	2.99	1.22	59.11	384
S-6	260	42.0	75.4	85.4	39.9	15.4	4.00	1.78	55.60	557

[a] Reactions performed at 80ºC during 6 hours. [b] Reference runs. [c] Catalysts prepared by impregnation. [d] 1-Octene conversion. [e] TBHP conversion. [f] 1-octene selectivity towards epoxide. [g] TBHP use efficiency. [h] Turnover frequency. [i] Molybdenum content in the catalyst before reaction. [j] Molybdenum content in the catalyst after reaction. [k] Molybdenum leaching extent. [l] Molybdenum solubilized in the reaction media.

Table 3. Reutilization runs using sample S-1 [a]

Run	Catalytic Results						Molybdenum stability			
	Oct:Mo (molar)	**X_{Octene} (%)**	**X_{TBHP} (%)**	**S_{Epox} (%)**	**η_{TBHP} (%)**	**TOF (h^{-1})**	**Mo_0 (%)**	**Mo_f (%)**	**Mo_{Leach} (%)**	**Mo_{sol} (ppm)**
1st	1100	46.8	57.7	98.6	67.1	87.4	0.90	0.50	44.80	128
2nd	2050	42.7	41.8	99.7	86.9	146.5	0.50	0.40	22.15	36
3rd	2650	42.5	35.8	>99.9	97.5	187.2	0.40	0.40	---	0

[a] Reactions performed at 80ºC during 6 hours. For legend see table 2.